Two-Dimensional Layered Double Hydroxide Derived from Vermiculite Waste Water Supported Highly Dispersed Ni Nanoparticles for CO Methanation

Panpan Li [1], Mingyuan Zhu [1], Zhiqun Tian [2], Yang Han [1], Yu Zhang [3], Tuantuan Zhou [3], Lihua Kang [1], Jianming Dan [1], Xuhong Guo [1,4], Feng Yu [1,*], Qiang Wang [1,3,*] and Bin Dai [1,*]

[1] Key Laboratory for Green Processing of Chemical Engineering of Xinjiang Bingtuan, School of Chemistry and Chemical Engineering, Shihezi University, Shihezi 832003, China; ppl_19910109@163.com (P.L.); zhuminyuan@shzu.edu.cn (M.Z.); llccnn@stu.shzu.edu.cn (Y.H.); kanglihua@shzu.edu.cn (L.K.); djm_tea@shzu.edu.cn (J.D.); guoxuhong@ecust.edu.cn (X.G.)

[2] Collaborative Innovation Center of Renewable Energy Materials, Guangxi University, Nanning 530004, China; tianzhiqun@gxu.edu.cn

[3] Environmental Functional Nanomaterials (EFN) Laboratory, College of Environmental Science and Engineering, Beijing Forestry University, Beijing 100083, China; hjzhangyu@bjfu.edu.cn (Y.Z.); ztuant86@126.com (T.Z.)

[4] State Key Laboratory of Chemical Engineering, East China University of Science and Technology, Shanghai 200237, China

* Correspondence: yufeng05@mail.ipc.ac.cn (F.Y.); qiangwang@bjfu.edu.cn (Q.W.); db_tea@shzu.edu.cn (B.D.); Tel.: +86-993-2057277 (F.Y. & Q.W. & B.D.)

Abstract: Expanded multilayered vermiculite (VMT) was successfully used as catalyst support and Ni/VMT synthesized by microwave irradiation assisted synthesis (MIAS) exhibited excellent performance in our previous work. We also developed a two-dimensional porous SiO_2 nanomesh (2D VMT-SiO_2) by mixed-acid etching of VMT. Compared with three-dimensional (3D) MCM-41, 2D VMT-SiO_2 as a catalyst support provided a superior position for implantation of NiO species and the as-obtained catalyst exhibited excellent performance. In this paper, we successfully synthesized a layered double hydroxide (LDH) using the spent liquor after mixed-acid etching of VMT, which mainly contained Mg^{2+} and Al^{3+}. The as-calcined layered double oxide (LDO) was used as a catalyst support for CO methanation. Compared with Ni/MgAl-LDO, Ni/VMT-LDO had smaller active component particles; therefore, in this study, it exhibited excellent catalytic performance over the whole temperature range of 250–500 °C. Ni/VMT-LDO achieved the best activity with 87.88% CO conversion, 89.97% CH_4 selectivity, and $12.47 \times 10^{-2} \cdot s^{-1}$ turn over frequency (TOF) at 400 °C under a gas hourly space velocity of 20,000 mL/g/h. This study demonstrated that VMT-LDO as a catalyst support provided an efficient way to develop high-performance catalysts for synthetic natural gas (SNG) from syngas.

---

1. Introduction

Since carbon oxide methanation was discovered by Sabatier and Senderens in 1902, it has been well developed and widely used due to its capability as a chemical storage for excess H_2 generated from renewable energy and a solution for greenhouse gas recycling [1–3]. Synthetic natural gas (SNG) via methanation can result in the clean utilization of coal and biomass, and this can prove to be an

ideal method to solve the problem of the lack of natural gas in China [4,5]. In addition, methanation of carbon monoxide can also guarantee energy supplies, an important advantage owing to the increasing energy demand that accompanies the rapid development of the world economy.

Al_2O_3 has been one of the most commonly used catalyst supports due to its large specific surface area and moderate active component–support interaction [6]. The performance of an Al_2O_3-based catalyst is quite sensitive to the preparation method; catalysts prepared using solution combustion synthesis and the single-step sol-gel method can reduce the catalysts' disadvantages, such as sintering of Ni particles, facile carbon deposition, and severe sulfur poisoning at high temperature [7–11]. MgO as a promoter can also improve resistance to carbon deposition and minimize Ni particle sintering [12]. The Ni/MgO catalyst has a strong interaction between Ni and MgO, and MgO can depress the aggregation of Ni metal particles, leading to higher thermal stability and better performance [13,14].

2D materials have excellent electronic properties and exceptional mechanical robustness, and are favorable to be used as catalyst supports [15]. As a kind of 2D material, layered double hydroxide (LDH) with the advantages of unique structure, composition diversity, high stability, easy preparation, and low cost has shown great potential in the design and synthesis of novel supported catalysts. LDH has been widely employed in the synthesis of Ni-based catalysts with a high degree of dispersion and stability by utilization of anchoring effects to enhance the immobilization of the active phase [16,17]. Ni–Al LDHs are found to be promising catalyst precursors for CO_2 methanation reaction, and Ni/Al_2O_3-LDO can decrease the CO_2 methanation reaction temperature to 260 °C due to its high dispersion of Ni, and Fe(III) can further decrease the Ni particle size, resulting a higher catalytic performance of 58.2% methane yield at 220 °C [7,18]. MgAl-LDH has been used as a catalyst support in oxidation reactions [19,20], and the as-calcined samples, named layered double oxide (LDO) or mixed metal oxides (MMO) are also used as supports due to their large specific surface area and the strong interaction between active components and the support [16]. Li et al. [21] found that the NiMgAl-LDO catalyst showed excellent CO methanation performance in high-temperature region: 400–650 °C, the transmission electron microscopy (TEM) and X-ray diffraction (XRD) results indicated that upon calcination of the NiMgAl-LDH precursor, the NiO phase gains a strong interaction with MgO and/or Al_2O_3 to form a $Ni_xMg_{1-x}O$ solid solution, leading to high-temperature stability and high Ni dispersion. Fan et al. [12] used Mg–Al oxide-supported Ni catalysts which not only have excellent thermal stability at high temperature, but also showed catalytic activity at low temperature of 250 °C with a Ni loading of 40 wt %, which is ascribed to the large specific surface area and strong metal—support interaction. Buelens et al. [22] developed a "super-dry" CH_4 reforming through Le Chatelier's principle reaction using Ni/$MgAl_2O_4$ as a CH_4-reforming catalyst. In this reaction Fe_2O_3/$MgAl_2O_4$ was used as a solid oxygen carrier and oxidized CH_4 into CO_2 and H_2O, while the Fe_2O_3 reduced to Fe; CaO/Al_2O_3 as a CO_2 sorbent formed $CaCO_3$, then the $CaCO_3$ decomposed into CaO and CO_2, and CO_2 reduced to CO by Fe through a redox reaction. Compared with conventional dry reforming, "super-dry" CH_4 reforming can result in higher CO production, and showed both practical and economic benefits.

We have developed a type of 2D porous SiO_2 nanomesh from a mixed-acid etching of 2D expanded multilayered vermiculite (EML-VMT). In this paper we synthesized a 2D VMT-LDH using the spent liquor, which contains Mg^{2+}, Al^{3+}, etc., with a Mg/Al molar ratio of 1.5:1 [23,24]. The spent liquor also contains a small amount of Fe^{2+} and Ca^{2+}. Fe as the best promoter, can combine with Ni to form enhanced methanation catalysts, and Ca can improve the dispersion of nickel [25–27]. The as-calcined 2D VMT-LDO was used as a catalyst support for CO methanation and Ni/VMT-LDO exhibited better catalytic performance than Ni/MgAl-LDO in the entire temperature range. This VMT-LDH catalyst support realized recycling utilization of the spent liquors, effectively preventing the metal ions in the spent liquors pollute the environment at the same time.

2. Results and Discussion

2.1. XRD, SEM, and TEM Characterization of LDHS and LDOS

From Figure 1a, MgAl-LDH and VMT-LDH presented the characteristic diffraction peaks of a well-crystallized LDH phase (JCPDS NO. 22-0452) at 2θ of 11.71°, 34.33°, 61.34°, and 62.68°, corresponding to the reflections of planes (001), (100), (110), and (111), respectively. The diffraction peaks indicated that the LDH was successfully synthesized by using the spent liquor after mixed dilute aqua regia solution etching of vermiculite. After calcining at 550 °C for 5 h in a muffle furnace, the as-obtained MgAl-LDO and VMT-LDO (Figure 1b) showed the characteristic diffraction peaks of MgO (JCPDS NO. 65-0476) at 2θ of 36.94°, 42.92°, and 62.30°, corresponding to crystal lattice indices of (111), (200), and (220), respectively. No peaks indicative of Al_2O_3 species was detected in either MgAl-LDO or VMT-LDO, these observations suggested that Al_2O_3 was in an amorphous state or that Al^{3+} ions became incorporated into MgO to form spinel phases, such as $MgAl_2O_4$ [28–30]. The SEM and TEM images of the as-obtained LDOs are displayed in Figure 2. The plate-like structure of VMT-LDO can be obviously seen in the TEM images. The stratified structure as perfect as MgAl-LDO, which is more evidence that VMT-LDH was successfully synthesized. The Brunauer–Emmett–Teller (BET) surface of MgAl-LDO and VMT-LDO were 177.3 m^2/g and 72.4 m^2/g respectively.
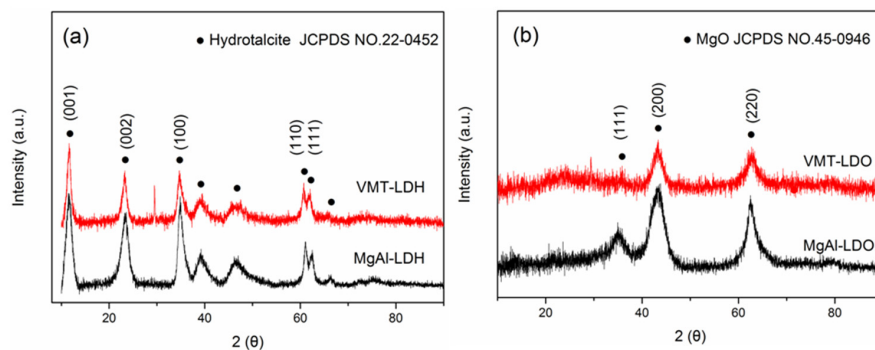

Figure 1. (**a**) X-ray diffraction (XRD) patterns of MgAl-LDH and VMT-LDH; (**b**) XRD patterns of MgAl-LDO and VMT-LDO.
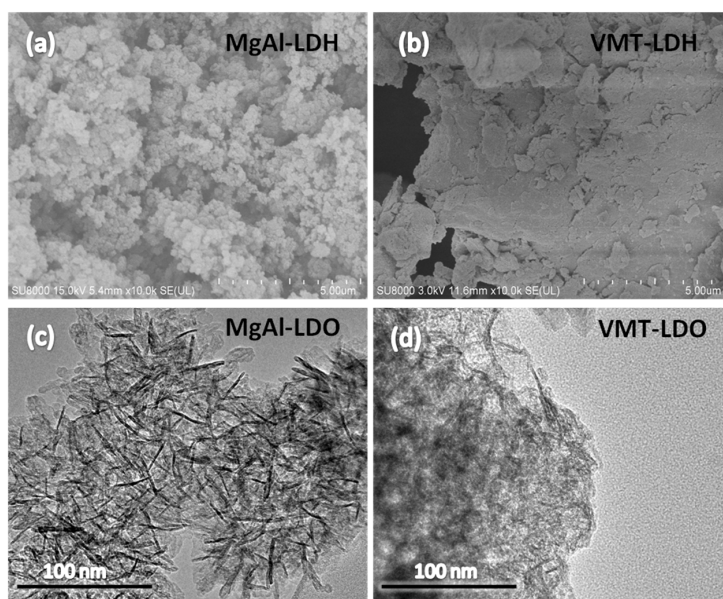

Figure 2. SEM images of (**a**) MgAl-LDH; (**b**) VMT-LDH; TEM images of (**c**) MgAl-LDO and (**d**) VMT-LDO.

2.2. XRD and TEM Characterization of Catalysts

Wide-angle XRD patterns of the as-calcined catalysts are shown in Figure 3a. Characteristic peaks of NiO (JCPDS NO. 65-5745) were distinctly observed at 2θ of 37.25°, 43.27°, and 62.88° for catalysts NiO/MgAl-LDO and NiO/VMT-LDO, corresponding to the reflections of planes (111), (200), and (220), respectively. Figure 3c, d show TEM images of the catalysts, as well as the surrounding structures. It can be seen clearly that the particle sizes of NiO/MgAl-LDO were larger than those of NiO/VMT-LDO. The majority of active component particles of NiO/ MgAl-LDO were around 20 nm in size, and the average NiO particle size obtained from TEM images was 18.1 nm. Whereas for NiO/VMT-LDO, the NiO particle size was around 2 nm, and the average NiO particle size was 2.3 nm, which indicated that the Ca and Fe modification might be able to improve the dispersion of nickel [18,25]. The specific surface areas of all samples are displayed in Table 1, and the catalysts NiO/MgAl-LDO and NiO/VMT-LDO gave areas of 52.5 m^2/g and 53.1 m^2/g, respectively.
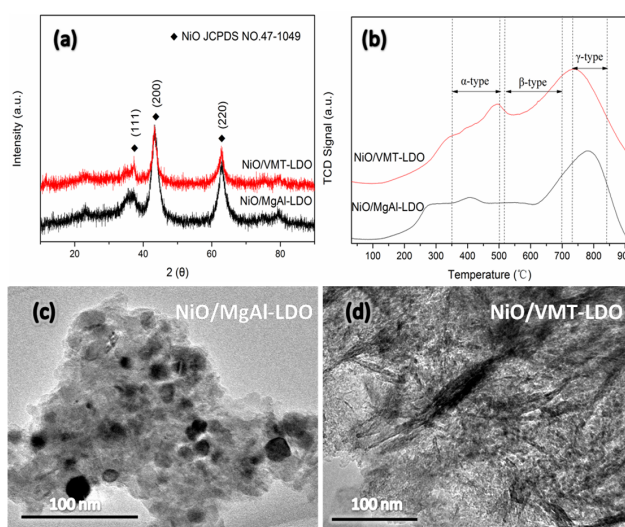

Figure 3. (**a**) XRD patterns of NiO/MgAl-LDO, NiO/VMT-LDO; (**b**) TPR profiles of NiO/MgAl-LDO and NiO/VMT-LDOTEM images of (**c**) NiO/MgAl-LDO and (**d**) NiO/VMT-LDO.

Table 1. Structural physical properties of the supports and catalysts.

Samples	S_{BET} (m$^2 \cdot$g^{-1}) [a]	Pore Volume (cm$^3 \cdot$g^{-1}) [b]	Pore Size (nm) [b]
MgAl-LDO	177.3	0.76	14.90
NiO/MgAl-LDO	52.5	0.15	3.91
Ni/MgAl-LDO (used)	45.0	0.22	24.98
VMT-LDO	72.4	0.16	7.36
NiO/VMT-LDO	53.2	0.22	5.63
Ni/VMT-LDO (used)	46.2	0.20	3.91

[a] Obtained from the Brunauer–Emmett–Teller (BET) method. [b] Obtained from the Barrett–Joyner–Halenda (BJH) desorption average pore volume and pore diameter.

2.3. TPR Characterization of Catalysts

The surface state and the reduction behavior of the catalysts NiO/VMT-LDO and NiO/MgAl-LDO were analyzed by H$_2$-TPR measurement (Figure 3b). There were three reduction peaks of NiO species observed in the H$_2$-TPR profile, which could be classified into three types: free nickel oxides possessing a weak interaction with the support (350–500 °C, α-type); NiO species that have a stronger interaction with the support (520–700 °C, β-type); the reduction peaks of MgNiO$_2$ solid solution (730–850 °C, γ-type) [10,21]. The first two reduction temperatures of NiO/VMT-LDO were centered at 338 °C and 491 °C, respectively. While the first two peaks' reduction temperatures of NiO/MgAl-LDO

were centered at 284 °C and 410 °C, respectively. The reduction temperatures of NiO/VMT-LDO were slightly higher than those of NiO/MgAl-LDO, suggesting that the interaction between NiO particles and VMT-LDO was stronger than that in MgAl-LDO. However, all of the reduction temperatures were below 500 °C, which meant that they belong to the α-type and could be reduced to generate active sites during the pretreatment before reaction. $MgNiO_2$ solid solution could not be reduced in pretreatment or during the reaction due to the strong interaction between Ni and MgO, resulting in a higher thermal stability [13].

2.4. Catalytic Performance of Catalysts

The CO methanation performance of the catalysts were carried out in the temperature range 250 °C–500 °C, as shown in Figure 4a. Ni/MgAl-LDO had shown no activity below 350 °C, and when the reaction temperature reached 400 °C, the catalyst Ni/MgAl-LDO showed 79.5% CO conversion, and the catalytic performance had shown no decline at the higher temperature. For Ni/VMT-LDO, the catalyst not only showed low-temperature activity at 250 °C, but also exhibited better catalytic performance than Ni/MgAl-LDO over the whole temperature range, reaching a maximum CO conversion of 87.9% at 400 °C, additionally. The higher catalytic performance was no doubt due to the smaller and higher dispersion of active components particle size. The trend of CH_4 selectivity (Figure 4b) for Ni/MgAl-LDO was in good agreement with that of CO conversion for Ni/MgAl-LDO in the temperature region: 250 °C–400 °C, and declined with the temperature, which resulted from the carbon deposition and the agglomeration of the active Ni component. When it came to the catalyst Ni/VMT-LDO, which showed an interesting curve of CH_4 selectivity, the CH_4 selectivity of Ni/VMT-LDO declined at 350 °C compared with 300 °C. Both samples obtained a maximum CH_4 selectivity at 400 °C. See Table 2 for a comparison of catalytic performance in different works.

It can be clearly seen in Figure 4c that Ni/VMT-LDO exhibited a higher turnover frequency (TOF) than Ni/MgAl-LDO over the whole temperature range. Ni/VMT-LDO reached a maximum TOF of $12.47 \times 10^{-2} \cdot s^{-1}$ at 400 °C, while for Ni/MgAl-LDO, a TOF value of $11.29 \times 10^{-2} \cdot s^{-1}$ was achieved at the same temperature. The highest TOF value of Ni/MgAl-LDO catalyst was $11.57 \times 10^{-2} \cdot s^{-1}$ at 500 °C. Ni/VMT-LDO also achieved a higher CH_4 yield in the whole temperature range compared with the catalyst Ni/MgAl-LDO (Figure 4d), the highest CH_4 yield was obtained at 400 °C for both samples. When the reaction temperature was higher than 400 °C, the CH_4 yield decreased with the temperature increased. However, Ni/MgAl-LDO and Ni/VMT-LDO still have ≥ 70% CH_4 yield at 500 °C. All of these results indicate that the catalytic performance of Ni/VMT-LDO catalyst was much better than that of Ni/MgAl-LDO catalyst.
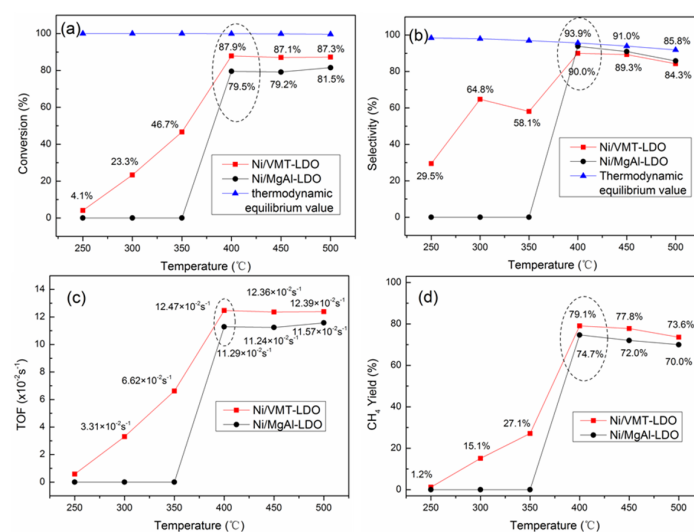

Figure 4. (**a**) CO conversion; (**b**) CH_4 selectivity; (**c**) turnover frequency (TOF) and (**d**) CH_4 yield of Ni/MgAl-LDO and Ni/VMT-LDO.

Table 2. The comparison of catalytic performance in different works.

Catalysts	Optical Temperature (°C)	Pressure (MPa)	Space Velocity (mL/g/h)	CO/CO$_2$ Conversion (%)	CH$_4$ Selectivity (%)	Ref.
40 wt % NiMgAl-LDO	250	0.1	40,000	98.4 (CO$_2$ + CO)	100	[12]
78 wt % NiAl-LDO	350	0.1	75,000	82.5 (CO$_2$)	99.5	[30]
NiAl-LDO(NiAl$_4$)	400	0.1	300,000	100 (CO)	92	[17]
11 wt % NiMgAl-LDO	400	-	15,000 h^{-1}	99.9 (CO)	73.6	[21]
10 wt % Ni/MgAl-LDO	400	1.5	20,000	79.5 (CO)	93.9	this work
10 wt % Ni/VMT-LDO	400	1.5	20,000	87.9 (CO)	90.0	this work

2.5. TEM and XRD Characterization of the Used Catalysts

　　After reaction, as shown in Figure 5, both catalysts Ni/MgAl-LDO (used) and Ni/VMT-LDO (used) exhibited no obvious agglomeration, and especially for catalyst Ni/VMT-LDO (used) there were no obvious Ni particles to be seen, the absence of Ni particles in the catalysts being due to the smaller Ni particles and the formation of Ni–Mg solid solutions [21]. XRD patterns of the used catalysts are shown in Figure 6. For Ni/MgAl-LDO (used) and Ni/VMT-LDO (used), both samples showed the diffraction peaks of metal Ni (JCPDS NO. 65-0380) at 2θ of 44.35°, 51.67°, and 76.09°. Diffraction peaks of MgNiO$_2$ (JCPDS NO. 24-0712) could also be seen at 2θ of 37.10°, 43.10°, and 62.59°, which was another argument in favor of the formation of Ni–Mg solid solutions. The MgNiO$_2$ solid solution inhibited the agglomeration of Ni nanoparticles, which maintained high CO conversion and thermal stability at high temperatures. However, for Ni/MgAl-LDO (used), the diffraction peaks of spinel (MgAl$_2$O$_4$) could be observed at 2θ of 19.03°, 31.27°, 36.85°, 44.83°, 55.66°, 59.37°, and 65.24°, suggesting spinel (MgAl$_2$O$_4$) formation during the reaction. Spinel could promote catalytic performance, leading to enhanced reactivity with increasing temperature [12,31].
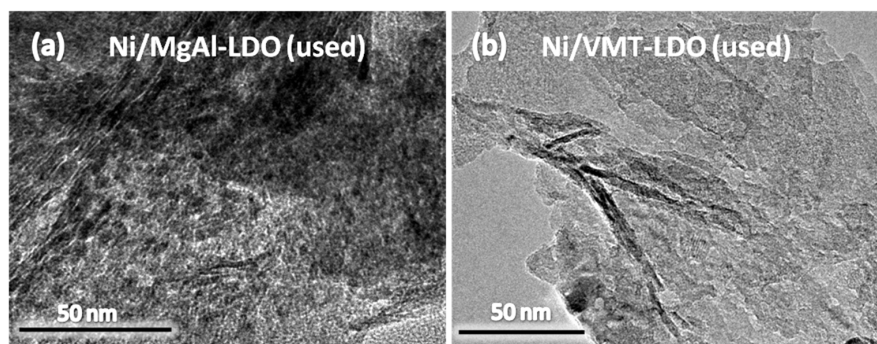
Figure 5. TEM images of (**a**) Ni/MgAl-LDO (used) and (**b**) Ni/ VMT-LDO (used).
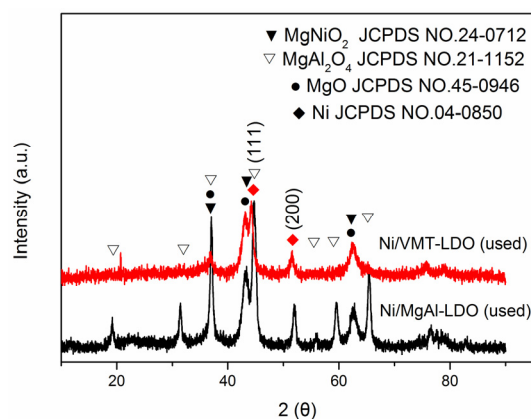
Figure 6. X-ray diffraction pattern of Ni/MgAl-LDO (used) and Ni/ VMT-LDO (used).

3. Materials and Methods

3.1. Catalyst Preparation

The procedure to prepare expanded multilayered vermiculite (EML-VMT) followed the protocol as described in our previous work [24]. The schematic of the preparation process of VMT-LDH is displayed in Figure 7, vermiculite was expanded by H_2O_2 to obtain the EML-VMT, then the EML-VMT was etched with acid to remove SiO_2. Subsequently the spent liquor was used to prepare LDH. The LDO was obtained by calcination of LDH, and then the catalyst was prepared through the impregnation method.

Specific steps to prepare the LDH using the spent liquor are as follows: a 200 mL portion of 6 M mixed acid solution (hydrochloric acid and nitric acid with volume ratio of 3:1) was placed into round-bottom flask equipped with a reflux condenser. Ten grams of EML-VMT was added and boiled in the flask at 80 °C for 4 h with constant stirring. The obtained samples were filtered. The filtrate, which mainly contained Mg^{2+} and Al^{3+}, was collected and neutralized by adding 4 M NaOH until precipitates started to appear in the solution. Then, the filtrate solution was added dropwise to Na_2CO_3 solution (100 mL) containing 0.04 mol Na_2CO_3, the pH value of the mixture was kept constant at 10 by addition of 4 M NaOH and then the solution was aged at room temperature for 4 h with continuous stirring. Afterwards, the mixture was filtered and washed with deionized water until pH = 7 and then dispersed with acetone for 2 h. The sample was filtered and washed with acetone again and then left to dry at 60 °C in an oven. The as-obtained support was denoted as VMT-LDH. In comparison, the MgAl-LDH with an Mg/Al molar ratio of 1.5:1 was also synthesized. Then VMT-LDH and MgAl-LDH were calcined at 550 °C for 4 h, and the as-obtained layered double oxides named VMT-LDO and MgAl-LDO.
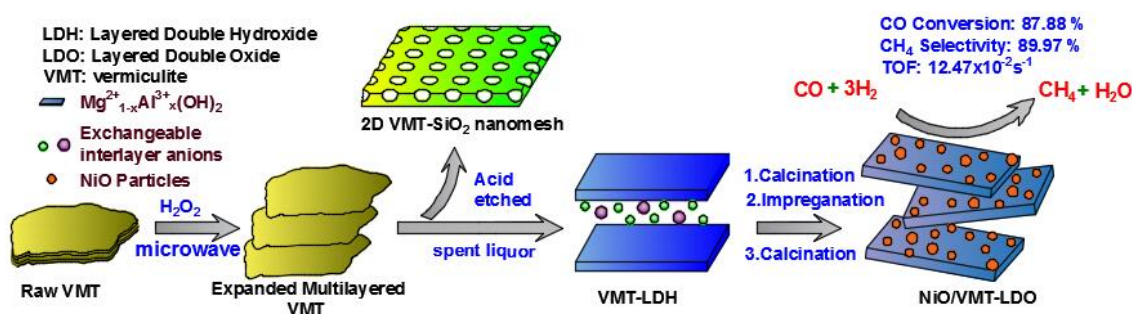

Figure 7. Schematic of the preparation process of VMT-LDH and NiO/VMT-LDH.

The catalyst was prepared using an impregnation method; the support (VMT-LDO or MgAl-LDO) was impregnated with an aqueous solution which contains certain quantities of $Ni(NO_3)_2 \cdot 6H_2O$ to achieve 10 wt % Ni loading, with vigorous stirring under the conditions of 80 °C for 12 h, and then evaporating the liquid. The as-prepared precursor was subsequently dried at 110 °C for 12 h and further calcined at 550 °C for 4 h in air at the heating rate of 10 °C/min. The obtained catalysts were denoted as NiO/VMT-LDO and NiO/MgAl-LDO.

3.2. Characterization of Samples

Powder X-ray diffraction (XRD) patterns were carried out on a Bruker D8 Advance X-ray diffractometer (Bruker Biosciences Corporation, Billerica, MA, USA) operated at 40 kV and 40 mA with Cu Kα radiation (λ = 0.15406 nm). The Brunauer–Emmett–Teller (BET) specific surface area and Barrett–Joyner–Halenda (BJH) pore structure of the catalysts were evaluated using a Micromeritics ASAP 2020 BET apparatus (Micromeritics Instrument Ltd., Norcross, GA, USA). The Micromeritics TPx System (Micromeritic ASAP 2720, Micromeritics Instrument Ltd., Norcross, GA, USA) was also employed to analysis the H_2 temperature programmed reduction (H_2-TPR) properties of catalysts

in a temperature range from room temperature to 900 °C, with a gas (10 vol % H_2/Ar) flow rate of 40 mL/min and a heating rate of 10 °C/min. Scanning electron microscopy (SEM) (Hitachi S-4300, Hitachi Limited, Japan) and transmission electron microscopy (TEM) (TecnaiG2 F20, FEI Instrument Ltd., Hillsboro, OR, USA) were employed to observe the microscopic of the catalysts.

3.3. Catalytic Performance Evaluation

The evaluation of CO methanation performance of the catalysts were performed in a fixed bed reactor at 1.5 Mpa, with a stainless steel tubular microreactor. Prior to the feed syngas H_2/CO with a volume ratio of 3:1 was introduced to the reactor, the catalyst (0.2 g) was activated in 28 mL/min H_2 at 500 °C for 2 h. Then the feed syngas introduced to the reactor with a gas flow rate of 65 mL/min and a weight space velocity of 20,000 mL/g/h, and the catalytic performance of the catalysts were evaluated in the temperature region of 250–500 °C. The outlet gases were analyzed by gas chromatography (GC-2014C, SHIMADZU) (GC-2014C, Shimadzu, Kyoto, Japan) online.

4. Conclusions

In this work, layered double hydroxide (LDH) was successfully synthesized, and the as-calcined layered double oxide (LDO) was used as a support for CO methanation. The as-obtained catalyst Ni/VMT-LDO had smaller Ni nanoparticles compared with catalyst Ni/MgAl-LDO, which was ascribed to Fe and Ca modification improved the dispersion of nickel, which resulted in a low temperature activity. The stronger metal–support interaction between Ni and VMT-LDO maintained the higher catalytic performance than the catalyst Ni/MgAl-LDO at higher temperature, so it was no doubt that the catalyst Ni/VMT-LDO exhibited excellent catalytic performance and thermal stability over the whole temperature range. Compared with Ni/MgAl-LDO, Ni/VMT-LDO achieved a better catalytic performance at 400 °C, including a 87.88% CO conversion, 89.97% CH_4 selectivity, $12.47 \times 10^{-2} \cdot s^{-1}$ turn over frequency (TOF) and 79.1% CH_4 yield. This study demonstrated that VMT-LDO was a superior catalyst support to develop a catalyst for synthesis of SNG from syngas, and the VMT-LDO which contains Fe and Ca can also be used as catalyst support in other catalytic systems, such as super-dry reformation of methane.

Author Contributions: Feng Yu, Qiang Wang, and Bin Dai designed and conceived the experiments; Panpan Li, Yang Han, Yu Zhang, and Tuantuan Zhou performed the experiments, Panpan Li, Mingyuan Zhu, Zhiqun Tian, Lihua Kang, Jianming Dan, and Xuhong Guo analyzed the data; Panpan Li and Feng Yu wrote the paper. All authors participated in the analysis, interpretation, and review of the results and provided input in the writing process of the paper.

Conflicts of Interest: The authors declare no conflict of interest.

References

1. Centi, G.; Quadrelli, E.A.; Perathoner, S. Catalysis for CO_2 conversion: A key technology for rapid introduction of renewable energy in the value chain of chemical industries. *Energy Environ. Sci.* **2013**, *6*, 1711–1731. [CrossRef]

2. Cheng, D.D.; Negreiros, F.R.; Aprà, E.; Fortunelli, A. Computational approaches to the chemical conversion of carbon dioxide. *ChemSusChem* **2013**, *6*, 944–965. [CrossRef] [PubMed]

3. Sabatier, P.; Senderens, J. New Synthesis of Methane. *Comptes Rendus Hebdomadaires des Seances del Academie des Scrences* **1902**, *134*, 514–516.

4. Kopyscinski, J.; Schildhauer, T.J.; Biollaz, S.M.A. Production of synthetic natural gas (sng) from coal and dry biomass—A technology review from 1950 to 2009. *Fuel* **2010**, *89*, 1763–1783. [CrossRef]

5. Seemann, M.C.; Schildhauer, T.J.; Biollaz, S.M.A. Fluidized bed methanation of wood-derived producer gas for the production of synthetic natural gas. *Ind. Eng. Chem. Res.* **2010**, *49*, 7034–7038. [CrossRef]

6. Hu, D.; Gao, J.; Ping, Y.; Jia, L.; Gunawan, P.; Zhong, Z.; Xu, G.; Gu, F.; Su, F. Enhanced investigation of CO methanation over Ni/Al$_2$O$_3$ catalysts for synthetic natural gas production. *Ind. Eng. Chem. Res.* **2012**, *51*, 1254–1262. [CrossRef]

7. Gabrovska, M.; Edreva-Kardjieva, R.; Crişan, D.; Tzvetkov, P.; Shopska, M.; Shtereva, I. Ni–Al layered double hydroxides as catalyst precursors for CO$_2$ removal by methanation. *React. Kinet. Mech. Catal.* **2012**, *105*, 79–99. [CrossRef]

8. Mirodatos, C.; Praliaud, H.; Primet, M. Deactivation of nickel-based catalysts during CO methanation and disproportionation. *J. Catal.* **1987**, *107*, 275–287. [CrossRef]

9. Struis, R.P.W.J.; Schildhauer, T.J.; Czekaj, I.; Janousch, M.; Biollaz, S.M.A.; Ludwig, C. Sulphur poisoning of Ni catalysts in the sng production from biomass: A TPO/XPS/XAS study. *Appl. Catal. A Gen.* **2009**, *362*, 121–128. [CrossRef]

10. Zhao, A.; Ying, W.; Zhang, H.; Ma, H.; Fang, D. Ni–Al$_2$O$_3$ catalysts prepared by solution combustion method for syngas methanation. *Catal. Commun.* **2012**, *17*, 34–38. [CrossRef]

11. Hwang, S.; Lee, J.; Hong, U.G.; Seo, J.G.; Ji, C.J.; Dong, J.K.; Lim, H.; Byun, C.; Song, I.K. Methane production from carbon monoxide and hydrogen over nickel–alumina xerogel catalyst: Effect of nickel content. *J. Ind. Eng. Chem.* **2011**, *17*, 154–157. [CrossRef]

12. Fan, M.T.; Miao, K.P.; Lin, J.D.; Zhang, H.B.; Liao, D.W. Mg-Al oxide supported Ni catalysts with enhanced stability for efficient synthetic natural gas from syngas. *Appl. Surf. Sci.* **2014**, *307*, 682–688. [CrossRef]

13. Bradford, M.C.; Vannice, M.A. Catalytic reforming of methane with carbon-dioxide over nickel-catalysts I. Catalyst characterization and activity. *Appl. Catal. A Gen.* **1996**, *142*, 73–96. [CrossRef]

14. Nakayama, T.; Ichikuni, N.; Sato, S.; Nozaki, F. Ni/MgO catalyst prepared using citric acid for hydrogenation of carbon dioxide. *Appl. Catal. A Gen.* **1997**, *158*, 185–199. [CrossRef]

15. Xu, Y.; Cheng, C.; Du, S.; Yang, J.; Yu, B.; Luo, J.; Yin, W.; Li, E.; Dong, S.; Ye, P. Contacts between two- and three-dimensional materials: Ohmic, schottky, and p-n heterojunctions. *ACS Nano* **2016**, *10*, 4895–4919. [CrossRef] [PubMed]

16. Feng, J.; He, Y.; Liu, Y.; Du, Y.; Li, D. Cheminform abstract: Supported catalysts based on layered double hydroxides for catalytic oxidation and hydrogenation: General functionality and promising application prospects. *Cheminform* **2015**, *46*, 5291–5319. [CrossRef]

17. Bian, L.; Wang, W.; Xia, R.; Li, Z. Ni-based catalyst derived from Ni/Al hydrotalcite-like compounds by the urea hydrolysis method for CO methanation. *RSC Adv.* **2015**, *6*, 677–686. [CrossRef]

18. Hwang, S.; Hong, U.G.; Lee, J.; Seo, J.G.; Baik, J.H.; Dong, J.K.; Lim, H.; Song, I.K. Methanation of carbon dioxide over mesoporous Ni–Fe–Al$_2$O$_3$ catalysts prepared by a coprecipitation method: Effect of precipitation agent. *J. Ind. Eng. Chem.* **2013**, *19*, 2016–2021. [CrossRef]

19. Mitsudome, T.; Noujima, A.; Mizugaki, T.; Jitsukawa, K.; Kaneda, K. Cheminform abstract: Supported gold nanoparticles as a reusable catalyst for synthesis of lactones from diols using molecular oxygen as an oxidant under mild conditions. *Green Chem.* **2009**, *11*, 793–797. [CrossRef]

20. Liu, P.; Li, P.C.; Hensen, P.E.J.M. Efficient tandem synthesis of methyl esters and imines by using versatile hydrotalcite-supported gold nanoparticles. *Chemistry* **2012**, *18*, 12122–12129. [CrossRef] [PubMed]

21. Li, Z.; Bian, L.; Zhu, Q.; Wang, W. Ni-based catalyst derived from Ni/Mg/Al hydrotalcite-like compounds and its activity in the methanation of carbon monoxide. *Kinet. Catal.* **2014**, *55*, 217–223. [CrossRef]

22. Buelens, L.C.; Galvita, V.; Poelman, H.; Detavernier, C.; Marin, G.B. Super-dry reforming of methane intensifies CO$_2$ utilization via le chatelier's principle. *Science* **2016**, *354*, 449–452. [CrossRef] [PubMed]

23. Dan, J.; Huang, X.; Li, P.; Zhang, Y.; Zhu, M.; Guo, X.; Dai, B.; Wang, Q.; Yu, F. Two-dimensional porous silica nanomesh from expanded multilayered vermiculite via mixed acid leaching. *Nanosci. Nanotechnol. Lett.* **2016**, *8*, 1028–1032. [CrossRef]

24. Li, P.; Wen, B.; Yu, F.; Zhu, M.; Guo, X.; Han, Y.; Kang, L.; Huang, X.; Dan, J.; Ouyang, F. High efficient nickel/vermiculite catalyst prepared via microwave irradiation-assisted synthesis for carbon monoxide methanation. *Fuel* **2016**, *171*, 263–269. [CrossRef]

25. Feng, Y.; Yang, W.; Chu, W. Effect of ca modification on the catalytic performance of Ni/AC for comethanation. *Integr. Ferroelectr.* **2016**, *172*, 40–48. [CrossRef]

26. Hwang, S.; Lee, J.; Hong, U.G.; Ji, C.J.; Dong, J.K.; Lim, H.; Byun, C.; Song, I.K. Hydrogenation of carbon monoxide to methane over mesoporous nickel-m-alumina (Fe, Ni, CO, Ce, and La) xerogel catalysts. *J. Ind. Eng. Chem.* **2012**, *18*, 243–248. [CrossRef]

27. Hwang, S.; Hong, U.G.; Lee, J.; Baik, J.H.; Dong, J.K.; Lim, H.; Song, I.K. Methanation of carbon dioxide over mesoporous Nickel–*M*–Alumina (*M* = Fe, Zr, Ni, Y, and Mg) xerogel catalysts: Effect of second metal. *Catal. Lett.* **2012**, *142*, 860–868. [CrossRef]

28. Fornasari, G.; Gazzano, M.; Matteuzzi, D.; Trifirò, F.; Vaccari, A. Structure and reactivity of high-surface-area Ni/Mg/Al mixed oxides. *Appl. Clay Sci.* **1995**, *10*, 69–82. [CrossRef]

29. Olsbye, U.; Akporiaye, D.; Rytter, E.; Rønnekleiv, M.; Tangstad, E. On the stability of mixed M^{2+}/M^{3+} oxides. *Appl. Catal. A Gen.* **2002**, *224*, 39–49. [CrossRef]

30. He, L.; Lin, Q.; Liu, Y.; Huang, Y. Unique catalysis of ni-al hydrotalcite derived catalyst in CO_2 methanation: Cooperative effect between ni nanoparticles and a basic support. *J. Energy Chem.* **2014**, *23*, 587–592. [CrossRef]

31. Kustov, A.L.; Frey, A.M.; Larsen, K.E.; Johannessen, T.; Nørskov, J.K.; Christensen, C.H. CO methanation over supported bimetallic Ni–Fe catalysts: From computational studies towards catalyst optimization. *Appl. Catal. A Gen.* **2007**, *320*, 98–104. [CrossRef]